ELSEVIER

Biophysical Chemistry 91 (2001) 79–91

Biophysical Chemistry

www.elsevier.nl/locate/bpc

Theoretical formalism for bead movement powered by single two-headed motors in a motility assay

Yi-der Chen*, Bo Yan

Mathematical Research Branch, National Institute of Diabetes and Digestive and Kidney Diseases, National Institutes of Health, Bethesda, MD 20892-2690 USA

Received 12 February 2001; received in revised form 20 March 2001; accepted 20 March 2001

Abstract

Kinesins and dyneins are protein motors that can use the free energy of ATP hydrolysis to carry a cargo and move uni-directionally along a microtubule filament. The purpose of this paper is to derive the formalism connecting the ATP-driven translocation reactions of these motors on microtubule filaments and the movement of the bead carried by the motor in a motility assay in which the bead is clamped at an arbitrary constant force. The formalism is thus useful in elucidating the load-dependent kinetic mechanism of the free-energy transduction of the motor using the mechanical data obtained from the motility assay. The formalism is also useful in assessing the effect on the measured motility data of various physical and hydrodynamic parameters of the assay, such as the size of the bead, the viscosity of the medium, the stiffness of the elastic element connecting the motor and the bead, etc. In a previous paper [Biophys. J. 67 (2000) 313] (hereafter referred to as paper I), we have derived the formalism for the case that the motor in the assay has only one head. In this paper we extend the derivation to the case that the motor is two-headed. The formalism is derived based on a simple two-state hand-over-hand model for the movement of the motor on microtubule, but can be easily extended to more complicated kinetic models. Effects of various hydrodynamic parameters on the velocity of the bead are studied with numerical calculations of the model. The difference between the formalism presented in this paper and the widely used 'chemical' formalism, in which the movement of the kinesin and the bead is described by pure chemical reactions, is discussed.

Keywords: Kinesin; Dynein; Free-energy transduction; Microtubule; Brownian motion

* Corresponding author. Tel.: +1-301-496-5436; fax: +1-301-402-0535.
E-mail address: ydchen@helix.nih.gov (Y. Chen).

0301-4622/01/$ - see front matter
PII: S0301-4622(01)00153-3

1. Introduction

Kinesins and dyneins are microtubule-based protein motors that can utilize the free energy of ATP hydrolysis to carry a cargo uni-directionally along a microtubule. Since the first kinesin was found in mid-1980, a number of different in vitro motility assays using purified motors have been developed in several laboratories to characterize the load-dependent free-energy transduction processes of these motors [2–10]. Mechanical properties, such as the step size, the velocity of movement of the motors, etc., have been elucidated from these motility measurements. Recently, Visscher et al. [10] have developed a motility assay in which the movement of a large plastic bead attached with a single purified kinesin motor can be measured under a force-clamp. With this assay, the velocity of the bead can be measured accurately as a function of the load at a fixed ATP concentration or as a function of ATP concentration at a fixed load. These motility data directly describe the relationship between the movement of the bead and the chemical driving force as a function of the externally applied load and should be useful in elucidating the mechanism of free energy transduction in kinesin motors. Up to now these motility data have been interpreted only in terms of the pure 'chemical' formalism, in which the movement of the motor is described by a set of chemical reactions with some force-dependent steps [11–16]. That is, the motion of the bead and its interaction with the motor are completely ignored and the force applied to the motor is assumed to be constant in this chemical formalism. However, since the motor is attached elastically to the bead in the motility assay and the movements of the bead and the motor are not synchronized, the motion of the bead should have a great influence on the kinetic reactions of the motor. Thus, it is important to consider the bead movement when the motility data of Visscher et al. [10] is used to elucidate the load-dependent kinetic mechanism of the motor.

In this series of studies, we present the derivation of formalisms that directly deal with the movement of the bead in the motility assay. Specifically, we derive formalisms that connect the movement of the bead in the motility assay of Visscher et al. and the kinetic reactions of ATP hydrolysis of the motor so that the measured motility data can be directly used for kinetic modeling. In paper I, we considered the system that the motor attached to the bead in the motility assay is one-headed. In this paper, we extend the derivation to the system that the motor is two-headed. We first derive the formalism using a simple two-state model with the hand-over-hand mechanism [17–20]. The effect of the various hydrodynamic parameters of the system on the bead velocity and the differences between the pure chemical formalism and the present formalism are then studied with some numerical calculations of the model. We show that with the same set of kinetic parameters the 'mean' velocity of the motor calculated without the interference of the bead (using the chemical formalism) is always larger than that with interference, unless the elastic element between the motor and the bead is completely flexible (with zero stiffness).

2. Mathematical formalism

We will derive the formalism based on the simple two-state kinetic model shown in Fig. 1a for the ATP hydrolysis-coupled translocation of a motor on a microtubule lattice. However, the derivation can be extended easily to other more complicated kinetic models. This model is a simplified version of the hand-over-hand model proposed for the processive movement of kinesin motor on microtubule [17–20]. As described in Fig. 1a, the motor is assumed to exist only in two biochemical states, state 1 and state 2, and one and only one of its two heads is attached to the microtubule at any given time. The head attaches perpendicularly to the microtubule axis when in state 1 and is tilted toward the forward-moving direction (toward the + end of the microtubule for + end moving kinesins and toward the − end for dyneins) when in state 2. There are two kinds of transitions between states 1 and 2: the α and the β transition. In the α transition, the same head of the motor remains attached to the same binding site on the microtubule. On the other

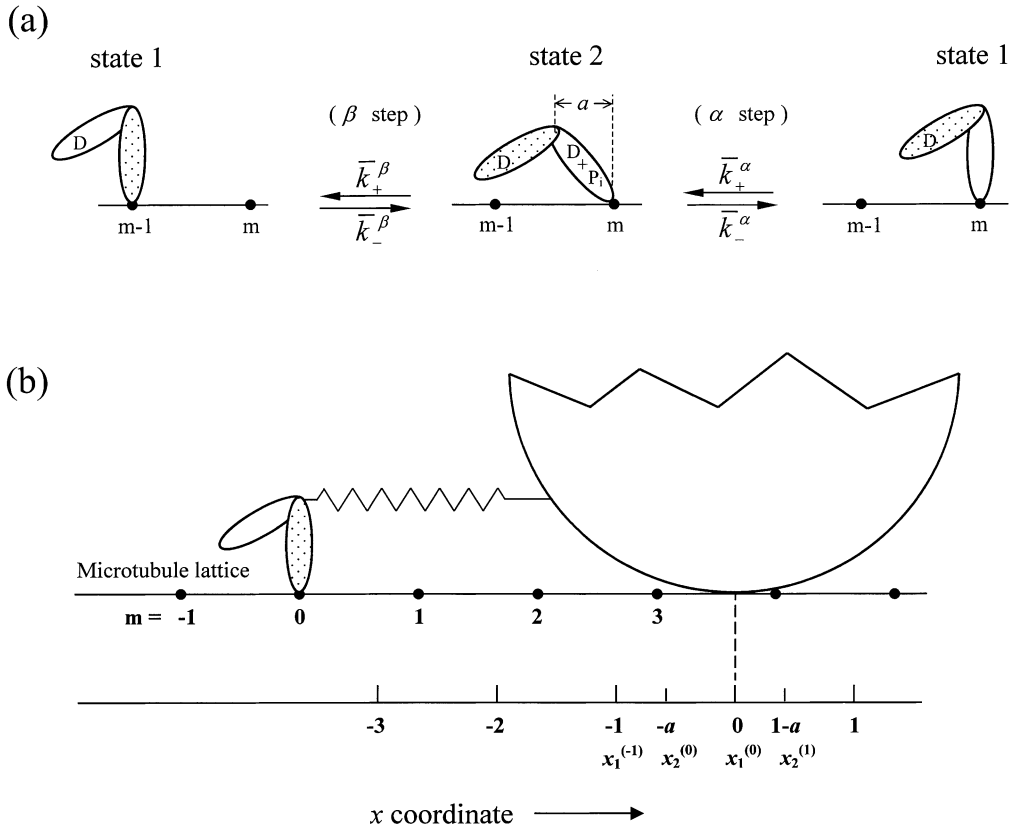

Fig. 1. (a) Schematic representation of the kinetic mechanisms of the two-state hand-over-hand model. The two-headed motor undergoes two 'power' strokes, α and β steps, when walking from site m to site $m-1$. The neck of the motor moves toward the left by a distance of a (normalized by dividing by the length of the lattice spacing, L) when a forward α step is executed and by a distance of $1-a$ when a forward β step is executed. Rate constant $\bar{k}_{+}^{\alpha}$ is proportional to the concentration of ATP and $\bar{k}_{-}^{\beta}$ is proportional to the concentrations of ADP and P_i. (b) The coordinate system (normalized by dividing by L) used to specify the position of the bead. The kinesin binding sites on the microtubule are labeled arbitrarily as $m=0, \pm1, \pm2, \ldots$ The origin of the coordinate system ($x=0$) is defined as the position of the bead on the microtubule (labeled with a x) when the elastic element between the bead and the motor is relaxed. $x_i^{(m)}(i=1,2)$ denotes the position of the bead when the motor is in state i is attached to the lattice site m and the elastic element is relaxed.

hand, one head is detached from the binding site while the other head is attached to the neighboring site at the same time when undergoing the β transition. Thus, as shown in Fig. 1a, a motor moves one step forward on the microtubule (from site m to site $m-1$) and hydrolyzes one molecule of ATP when it carries out a forward α transition followed by a forward β transition.

The schematic representation of the physical arrangement of the motor and the bead in the motility assay of Visscher et al. [10] is given in Fig. 1b, in which only part of the spherical bead is shown. As discussed in I and shown in Fig. 1b, we arbitrarily label the periodic lattice sites on a microtubule as $m=0, \pm1, \pm2...$ The *origin* ($x=0$) of the x-axis of the coordinate system is then defined as the *position of the bead* (not that of the motor) when the motor in state 1 (the perpendicular state) can attach to the site at $m=0$ without generating any strain in the elastic element (i.e. the elastic element is relaxed). In other words, the origin of the x-axis is determined by the position of the site on the microtubule assigned as $m=0$ and the resting length of the elastic

element connecting the bead to the motor. The coordinate of each lattice site on this x-axis will depend on the length of the elastic element. But, this information is not needed in the formalism (see below). When attached to the bead, the motor still undergoes the cyclic ATP hydrolysis reactions shown in Fig. 1a. But, in contrast to the free motor case, the rate constants of both α and the β transitions are no longer constant, but x-dependent.

Let us assume that the elastic element between the motor and the bead obeys Hooke's law. Then, the strain energy generated by the elastic element when the bead is at x and the motor in state i ($i = 1,2$) is attached to the lattice site m can be expressed as

$$E_i^{(m)}(x) = \frac{K}{2}(x - x_i^{(m)})^2, \quad i = 1,2, \tag{1}$$

where K is the combined stiffness of the elastic element and the motor (see below) and $x_i^{(m)}$ is the position of the bead on the x-axis when the motor is attached to the lattice site m in state i and the elastic element is relaxed (e.g. $x_1^{(0)} = 0$, $x_2^{(0)} = -a$, etc., see Fig. 1b). For convenience, the quantities $E_i^{(m)}$ and x are made dimensionless by dividing their physical quantities by $k_B T$ and L, respectively: $E_i^{(m)}(x) = \bar{E}_i^{(m)}(x)/k_B T$ and $x = \bar{x}/L$ where k_B is the Boltzmann constant, T is the absolute temperature, and L is the length of the lattice spacing (the length of a tubulin dimer in a microtubule protofilament). In this case, K is also dimensionless and is related to its corresponding physical quantity $\bar{K}$ as $K = \bar{K}L^2/k_B T$. As shown in Fig. 1b, in this normalized x coordinate system, $x_1^{(m)} = m$ and $x_2^{(m)} = m - a$ where a is the length increase (also in units of L) of the elastic element when a forward α transition is executed (see Fig. 1a). One must note that the motor is assumed to move forward to the negative x-axis. Thus, for (+)-end kinesins, the (+) end of the microtubule is pointing toward the negative x direction.

Let $\bar{\alpha}_+^{(m)}(x)$ and $\bar{\alpha}_-^{(m)}(x)$ represent the x-dependent forward (+) and backward (−) rate constants, respectively, of the α step in Fig. 1a when the motor is attached to site m and the bead is located at x and $\bar{\beta}_+^{(m)}(x)$ and $\bar{\beta}_-^{(m-1)}(x)$ be the corresponding rate constants of the β step between sites m and $m-1$. Then, as in paper I, we assume that these rate constants can be expressed as a function of $\bar{k}_+^{\alpha}$, etc., in Fig. 1a and the quantities $E_i^{(m)}$ in Eq. (1) as:

$$\bar{\alpha}_+^{(m)}(x) = \bar{k}_+^{\alpha} \exp\left[\delta_\alpha (E_1^{(m)}(x) - E_2^{(m)}(x))\right], \tag{2}$$

$$\bar{\alpha}_-^{(m)}(x) = \bar{k}_-^{\alpha} \exp\left[-(1-\delta_\alpha) \times (E_1^{(m)}(x) - E_2^{(m)}(x))\right], \tag{3}$$

$$\bar{\beta}_+^{(m)}(x) = \bar{k}_+^{\beta} \exp\left[\delta_\beta (E_2^{(m)}(x) - E_1^{(m-1)}(x))\right], \tag{4}$$

$$\bar{\beta}_-^{(m-1)}(x) = \bar{k}_-^{\beta} \exp\left[-(1-\delta_\beta) \times (E_2^{(m)}(x) - E_1^{(m-1)}(x))\right], \tag{5}$$

$$m = 0, \ \pm 1, \ \pm 2, \ldots,$$

where δ_α and δ_β are constants that determine the division of the elastic strain effect between the forward and the backward rate constants for the two steps, respectively. It is important to point out here that Eqs. (2)–(5) are not the only expressions for the x-dependent rate constants; many other forms of equations can be obtained. The exact forms of these rate constants depend on how the original multi-state model is contracted or reduced to the two-state model (see Appendix 1 of Hill [21]). However, the ratio of the two α's (and the two β's) must remain unchanged and is dictated by thermodynamics. It is also important to point out that the derivation of the formalism does not depend on the exact forms of these rate constants.

Now consider an ensemble of systems in which the bead is subjected to a constant external load ($\bar{F}$) in the positive x direction. Let $p_i^{(m)}(x,t)$ ($i = 1,2$) be the probabilities of finding systems in the ensemble, in which the bead is located at x at time t and the motor is attached to the lattice site

m in state i. Then, these probabilities obey the diffusion-reaction equations:

$$\frac{\partial p_1^{(m)}(x,t)}{\partial t} = -\frac{\partial u_1^{(m)}}{\partial x} + \beta_+^{(m+1)}(x)p_2^{(m+1)}(x,t) - (\beta_-^{(m)}(x) + \alpha_+^{(m)}) \times p_1^{(m)}(x,t) + \alpha_-^{(m)}(x)p_2^{(m)}(x,t), \quad (6)$$

$$\frac{\partial p_2^{(m)}(x,t)}{\partial t} = -\frac{\partial u_2^{(m)}}{\partial x} + \beta_-^{(m-1)}(x)p_1^{(m-1)}(x,t) - (\beta_+^{(m)}(x) + \alpha_-^{(m)}) \times p_2^{(m)}(x,t) + \alpha_+^{(m)}(x)p_1^{(m)}(x,t), \quad (7)$$

$m = 0, \pm 1, \pm 2, \ldots,$

where

$$u_i^{(m)} = -\frac{\partial p_1^{(m)}}{\partial x} - p_1^{(m)}\frac{\partial E_i^{(m)}}{\partial x} + Fp_i^{(m)}, \quad i = 1,2. \quad (8)$$

Note that the $\alpha_+^{(m)}$, etc., and F in Eqs. (6)–(8) are also dimensionless: $F = \bar{F}L/k_BT$ and $\alpha_+^{(m)} = \bar{\alpha}_+^{(m)}(x)L^2/D$, etc. where D is the diffusion coefficient of the bead.

Combining Eqs. (6) and (7) together and summing over m, we get

$$\frac{\partial p}{\partial t} = -\frac{\partial u}{\partial x} + \sum_{m=0,\pm1,\pm2,\ldots} \times \left[\beta_+^{(m+1)}p_2^{(m+1)} - \beta_-^{(m)}p_1^{(m)} + \beta_-^{(m-1)}p_1^{(m-1)} - \beta_+^{(m)}p_2^{(m)}\right], \quad (9)$$

where $p \equiv \sum_m (p_1^{(m)} + p_2^{(m)})$ and $u \equiv \sum_m (u_1^{(m)} + u_2^{(m)})$. It is easy to see that the last term in Eq. (9) becomes zero after carrying out the summation and recognizing that $p_1^{(m)}$ and $p_2^{(m)}$ tend to zero at large $|m|$. Thus, we have $\partial p(x,t)/\partial t = -\partial u/\partial x$. Then, at steady state u becomes a constant independent of x. This steady state u is equal to the *mean velocity* of the movement of the bead on the periodic lattice, if the sum of the steady-state probabilities within each period is equal to unity [1,22]. Thus, the key to evaluating the mean velocity of the bead in this system is to solve Eqs. (6) and (7) at steady state.

It is easy to see that at steady state the probabilities $p_i^{(m)}(x)$ at any m can be expressed in terms of those at $m = 0$ as

$$p_i^{(m)}(x) = p_i^{(0)}(x - m) \quad (10)$$

Since $x_1^{(m)} = m$ and $x_2^{(m)} = m - a$, Eq. (1) implies that $E_i^{(m)}(x) = E_i^{(0)}(x - m)$. In this case, the dimensionless rate constants in Eqs. (2)–(5) can also be expressed as those at $m = 0$ as:

$$\alpha_+^{(m)}(x) = \alpha_+^{(0)}(x - m), \text{ etc.} \quad (11)$$

With Eqs. (10) and (11), the differential equations in Eqs. (6) and (7) at steady state can be reduced to the following ordinary differential equations at $m = 0$:

$$\frac{d^2p_1(x)}{dx^2} + \frac{d}{dx}\left[p_1(x)\left(\frac{dE_1(x)}{dx} - F\right)\right] + \beta_+(x-1)p_2(x-1) - [\beta_-(x) + \alpha_+(x)]p_1(x) + \alpha_-(x)p_2(x) = 0 \quad (12)$$

$$\frac{d^2p_2(x)}{dx^2} + \frac{d}{dx}\left[p_2(x)\left(\frac{dE_2(x)}{dx} - F\right)\right] + \beta_-(x+1)p_1(x+1) - [\beta_+(x) + \alpha_-(x)]p_2(x) + \alpha_+(x)p_1(x) = 0 \quad (13)$$

where the superscript (0) in $E_i^{(0)}(x)$, $p_i^{(0)}(x)$, and $\alpha_+^{(0)}(x)$, etc., has been dropped for convenience.

Explicit expressions of $\alpha_+(x)$, etc., in Eqs. (12) and (13) can be obtained from Eqs. (1)–(5) as

$$\alpha_+(x) = k_+^{\alpha} e^{-Ka\delta_\alpha(2x+a)/2};$$
$$\alpha_-(x) = k_-^{\alpha} e^{Ka(1-\delta_a)(2x+a)/2},$$

$$\beta_+(x) = k_+^{\beta} e^{-K(1-a)\delta_\beta(2x+a+1)/2};$$
$$\beta_-(x) = k_-^{\beta} e^{K(1-a)(1-\delta_\beta)(2x+a-1)/2} \quad (14)$$

where $k_{+\alpha} \equiv \bar{k}_{+\alpha} L^2/D$, etc., is dimensionless.

In general, $p_1(x)$ and $p_2(x)$ are mostly populated near $x=0$ and are expected to decrease rather rapidly when $|x|$ increases. Thus, it is reasonable to assume that both p_1 and p_2 become negligible when $|x|$ is greater than some fixed value b. In other words, the differential equations in Eqs. (12) and (13) can be solved numerically between $x=-b$ and $x=b$ using the finite difference method [1,22] and the following boundary and normalization conditions:

$$p_1(\pm b) = p_2(\pm b) = 0 \quad (15)$$

$$\int_{-b}^{+b} [p_1(x) + p_2(x)]\mathrm{d}x = 1 \quad (16)$$

In general, the value of b used in numerical solutions is determined by the value of K: the smaller the K, the larger the b is required. For the calculations to be presented below with $K=16$ (see Table 1), a value of $b=3$ was found to be enough. Note a different numerical method for solving similar problems has been discussed before [23].

The mean velocity of the bead at steady state can be evaluated from the steady-state probabilities using the equation:

$$u = -\sum_{m=0,\pm1,\pm2,\ldots} \left\{ \frac{\mathrm{d}p_1(x-m)}{\mathrm{d}x} + p_1(x-m)[K\cdot(x-m) - F] + \frac{\mathrm{d}p_2(x-m)}{\mathrm{d}x} + p_2(x-m)[K\cdot(x-m+a) - F] \right\} \quad (17)$$

The mean ATP hydrolysis rate of the motor also can be evaluated from the probabilities either using the α step or the β step:

$$J_\alpha = \sum_{m=0,\pm1,\pm2,\ldots} \int_0^1 [\alpha_+(x-m)p_1(x-m) - \alpha_-(x-m)p_2(x-m)]\mathrm{d}x; \quad (18)$$

$$J_\beta = \sum_{m=0,\pm1,\pm2,\ldots} \int_0^1 [\beta_+(x-m)p_2(x-m) - \alpha_-(x-m-1)p_2(x-m-1)]\mathrm{d}x. \quad (19)$$

Since the movement of the motor on the microtubule is completely coupled to the ATP hydrolysis (no slippage), the ATP hydrolysis rate evaluated from Eq. (18) or Eq. (19) will equal to the mean velocity u evaluated from Eq. (17). One must note that u and J are dimensionless. The actual velocity of the bead and the ATP hydrolysis rate can be evaluated from these dimensionless quantities as $\bar{u} = uD/L$ and $\bar{J} = JD/L^2$. In other words, we have $\bar{u} = \bar{J}L$ in this tight-coupled system.

The basic part of the formalism is to solve the

Table 1
The reference set of parameters used in the calculations[a]

$D = 3\times10^{-9}$ cm^2 s^{-1}	$K = 16$
$L = 8$ nm	$a = 0.5$
$\delta_\alpha = 0.5$	$\delta_\beta = 0.13$
$\bar{k}_+^{\alpha} = 3.75\,[T]$ s^{-1}	$\bar{k}_-^{\alpha} = 3.4\times10^{-2}$ s^{-1}
$\bar{k}_+^{\beta} = 141.1$ s^{-1}	$\bar{k}_-^{\beta} = 4.7\times10^{-3}$ s^{-1}

[a] $[T]$ = concentration of ATP in μM.

two ordinary differential equations Eqs. (12) and (13) with the rate constants in Eq. (14) and the boundary conditions in Eqs. (15) and (16). In contrast to the one-headed case, the differential equations Eqs. (12) and (13) for the two-headed case do not contain the lattice site index, m. This is due to the fact that the motor cannot completely dissociate from the lattice in this hand-over-hand model. Note that these two differential equations can be extended readily to include the slippage steps in the kinetic mechanism of the model.

3. The 'chemical kinetic' formalism

In this section, we briefly describe how to calculate the velocity of the motor for the two-state hand-over-hand model in Fig. 1a based on the pure chemical formalism [11–16].

In this formalism, the dynamics of the bead is completely ignored so that the force applied to the motor is assumed to be constant and equal to the externally applied force. Then, using the same load-dependence in Eqs. (2)–(5), the load-dependent rate constants of the α and β steps in this formalism can be expressed in terms of the rate constants, $\bar{k}_+^\alpha$, etc., in Fig. 1a as: $\bar{k}_+^\alpha e^{-\bar{F}a\delta_\alpha}$, $\bar{k}_-^\alpha e^{\bar{F}a(1-\delta_\alpha)}$, $\bar{k}_+^\beta e^{-\bar{F}/(1-a)\delta_\beta}$, $\bar{k}_-^\beta e^{\bar{F}/(1-a)(1-\delta_\beta)}$, respectively [11,12]. With these rate constants, the velocity of the bead can be obtained as $\bar{u} = \bar{J}L$ where L is the length of the lattice spacing and $\bar{J}$ is the ATP hydrolysis cycle rate:

$$\bar{J} = \frac{[\bar{k}_+^\alpha \bar{k}_+^\beta - \bar{k}_-^\alpha \bar{k}_-^\beta e^{\bar{F}}] e^{\bar{F}[a(\delta_\beta - \delta_\alpha) - \delta_\beta]}}{\left[\bar{k}_+^\alpha e^{-\bar{F}a\delta_\alpha} + \bar{k}_+^\beta e^{-\bar{F}(1-a)\delta_\beta} + \bar{k}_-^\alpha e^{\bar{F}a(1-\delta_\alpha)} + \bar{k}_-^\beta e^{\bar{F}(1-a)(1-\delta_\beta)}\right]} \quad (20)$$

4. Illustrative model calculations

In this section, some numerical calculations are carried out for the two-state model in Fig. 1a defined by the rate constants in Eq. (14) and the parameters in Table 1. The purposes are: (1) to examine how the velocity of the bead in the assay is affected by the hydrodynamic parameters of the assay, such as the elastic coefficient of the elastic element K and the diffusion coefficient of the bead D; and (2) to examine the differences between the present formalism and the pure chemical formalism.

Table 1 lists the set of parameters of the model used in the calculation. The values of the parameters were chosen so that the calculated bead velocity as a function of ATP concentration is close to what measured by Visscher et al. [10] at $\bar{F} = 1.05$ and 5.63 pN (pico-Newton), respectively. Note that only the ATP concentration is explicitly expressed as a parameter in Table 1; the concentrations of ADP and P_i are assumed to be constant and are absorbed in the rate constant, $\bar{k}_-^\beta$. Also, note that the four rate constants in Fig. 1a were chosen so that, at the physiological condition ($[T] = 3$ mM), the thermodynamic relation, $\bar{k}_+^\alpha \bar{k}_+^\beta / \bar{k}_-^\alpha \bar{k}_-^\beta \approx e^{23}$, is satisfied [24,25] and the ATP hydrolysis rate in solution, $\bar{J} = (\bar{k}_+^\alpha \bar{k}_+^\beta - \bar{k}_-^\alpha \bar{k}_-^\beta)/(\bar{k}_+^\alpha + \bar{k}_+^\beta + \bar{k}_-^\alpha + \bar{k}_-^\beta)$, is approximately 100 s^{-1} [26].

4.1. Effect of the elastic coefficient K

Why are we interested in the effect of K and what is the value of K in a motility assay? In any in vitro motility assay, the motor is always 'glued' to something. In the bead movement assay, the motor is glued to the bead. In the microtubule-gliding assay, the motor is glued to a fixed surface. Thus, there is always some added elastic element in the system. In general, the elastic coefficient K in Eq. (1) contains contributions from the motor–microtubule complex and the elastic element between the bead and the motor. Let K_m and K_e be the elastic coefficients of the motor and the elastic element, respectively. Then, we have $K = K_m K_e/(K_m + K_e)$. Thus, K is always smaller than either K_m or K_e. If we assume $K_m = 16$ (corresponding to the elasticity of an actin–myosin cross-bridge in muscle [25], see the discussion in paper I), then $K = 16$ (as listed in Table 1) implies that the elastic element inserted between the motor and the bead is infinitely stiff.

If the elastic element has a finite value of elasticity, then the value of K is always smaller than the elastic coefficient of the motor. In general, in order to estimate the force generated by the motor from the motility assay, one needs to know the value of K_m and the elastic coefficient of the elastic element inserted between the motor and the bead.

The calculated bead velocity using the present formalism and the parameters in Table 1 is shown as a function of the stiffness K in Fig. 2a,b at $\bar{F} = 0$ (curves with filled circles) and 5.63 pN (curves with open circles) for [ATP] = 5 and 2000 μM, respectively. Also shown in the figures are the velocities of the bead calculated using the 'chemical' formalism (the dashed lines). For all cases, the calculated bead velocity $\bar{u}$ increases monotonically as the value of K decreases and is always smaller than that evaluated using the 'chemical' formalism, except at $K = 0$ where the two velocities become identical. This is not surprising, because the movement of the bead and the movement of the motor are completely uncoupled when $K = 0$.

However, the finding in the two-headed case that the bead velocity increases monotonically as K decreases is quite different from what we found for the one-headed kinesin case [1], in which the velocity increases at first, reaches a peak, and then decreases toward zero as K decreases. As discussed in paper I, for the one-headed kinesin case the increase in $\bar{u}$ depends on two factors: (1) the increase in the bias for the forward advancement of the motor along the microtubule; and (2) the increase in the ATP cycling rate. The ATP cycling rate increases as K decreases. This is the reason that $\bar{u}$ increases initially when K is reduced from a very large value. The increase in the bias for the forward movement of the motor requires the forward advancement of the bead. Thus, when K becomes very small so that the bead has no time to respond, the bias for the forward movement of the motor decreases. As a result, the bead velocity starts to decrease. For two-headed kinesins with the hand-over-hand mechanism, the motor does not dissociate from the microtubule. The forward movement of the motor along the microtubule is always biased; the bias does not depend on the forward advancement of the bead. Therefore, the velocity of the bead is simply proportional to the ATP cycling rate. Thus, when K decreases, the effect of the frictional drag of the bead on the ATP cycling rate decreases, resulting in a monotonic increase in ATP cycling rate and the velocity of the bead.

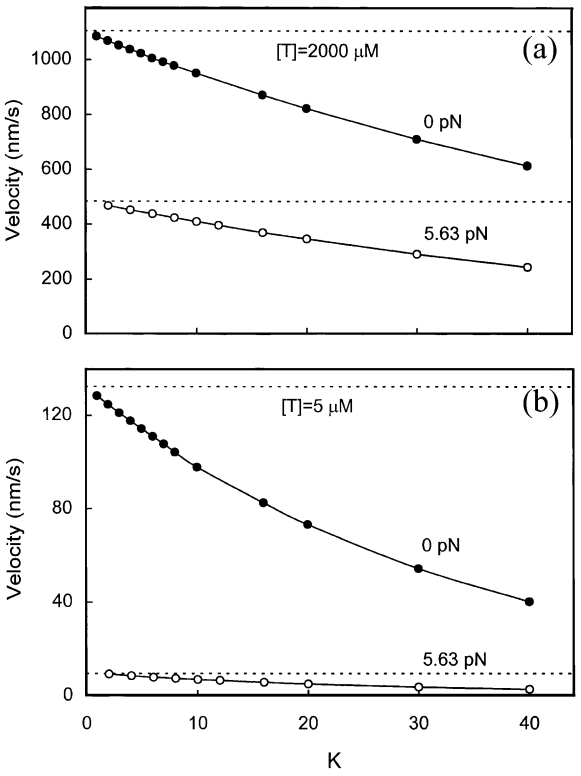

Fig. 2. The bead velocity as a function of the stiffness (K) of the elastic element calculated for the model using the parameters in Table 1 at (a) [ATP] = 2000 μM and (b) [ATP] = 5 μM, in the presence and absence of an external force applied to the bead. The dashed lines are those evaluated from Eq. (20) of the 'chemical' formalism without considering the involvement of the bead.

4.2. Effect of diffusion coefficient of the bead

In Fig. 3a, the calculated mean velocities of the bead ($\bar{u}$) are shown as a function of the diffusion coefficient of the bead for [ATP] = 2000 μM at $\bar{F} = 0$ and 5.63 pN and for [ATP] = 5 μM at $\bar{F} = 0$. In general, the bead velocity decreases

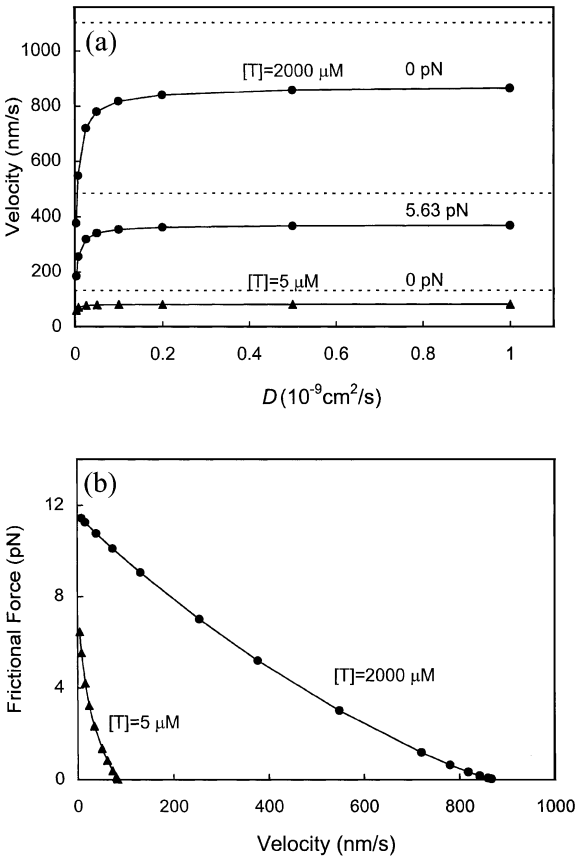

Fig. 3. (a) The calculated bead velocity as a function of the diffusion coefficient of the bead. The dashed lines are those from the chemical formalism. (b) The force–velocity curve obtained by plotting the product of the velocity and the diffusion coefficient (the frictional force of the bead) as a function of the velocity calculated in the absence of an external load ($\bar{F} = 0$).

slightly as the diffusion coefficient is decreased from the reference value of 3×10^{-9} cm^2 s^{-1} and pronounced decrease occurs only after D is reduced more than 10-fold. However, the external load $\bar{F}$ applied to the bead reduces the effect of D on the velocity. For example, the value of D at which the velocity starts to decrease sharply decreases as the externally applied load increases (compare the top two curves in Fig. 3a). Also the $\bar{u}(D)$ curve becomes flatter as the load increases. This is easy to understand, because when the external load is much larger than the frictional force of the bead, the effect of the diffusion coefficient of bead on the ATP cycling rate (and therefore the velocity of the bead) becomes negligible.

As shown in Fig. 3a, the velocity of the motor calculated based on Eq. (20) of the 'chemical' formalism is always larger than that calculated using the present formalism. The difference will be smaller, however, as the value of the K is decreased (see Fig. 2a,b).

The frictional force–velocity curve at $\bar{F} = 0$ (with no externally applied load) can be evaluated from the $\bar{u}(D)$ curves in Fig. 3a. The calculated force–velocity curve is shown in Fig. 3b for [ATP] $= 2000$ and 5 μM. The frictional force–velocity curve is slightly concave-upward, similar to that found in muscle. This is different from those measured by Hunt et al. [4], in which the force–velocity is approximately linear. As will be discussed below, the force–velocity curve evaluated by varying the diffusion coefficient of the bead at no external load is very similar to that obtained by directly applying an external force (load) to the bead.

By examining results in Fig. 2a,b, and Fig. 3a, we conclude: the more flexible the bead is (by increasing D or reducing K), the faster the bead moves at the same external load.

4.3. Effect of external load applied to the bead

By varying the value of F in Eqs. (12) and (13), the effect of a constant load on the bead movement can be studied. The load–velocity curve for the model with the parameters in Table 1 calculated at [ATP] = 2000 μM is shown in heavy line in Fig. 4a. Also shown in Fig. 4 are those calculated with reduced K or reduced D (dashed curves) and that calculated based on the chemical formalism (dotted line). Consistent with results in Fig. 2a,b, and Fig. 3a, the velocity evaluated based on the chemical formalism is always larger than that evaluated using the exact formalism at the same external load. It is also found that the frictional force–velocity curve obtained by varying the diffusion coefficient of the bead is identical to the force–velocity obtained by varying the external load applied to the bead (compare the upper

line in Fig. 3b with the heavy line in Fig. 4a). This result is quite different from what we found in paper I for the one-headed kinesin case: the frictional force is always larger than the externally applied load at the same bead velocity in the one-headed kinesin case.

The force applied to the bead at which the bead stops moving is called the 'stall' force. The stall force of a given system can be obtained from

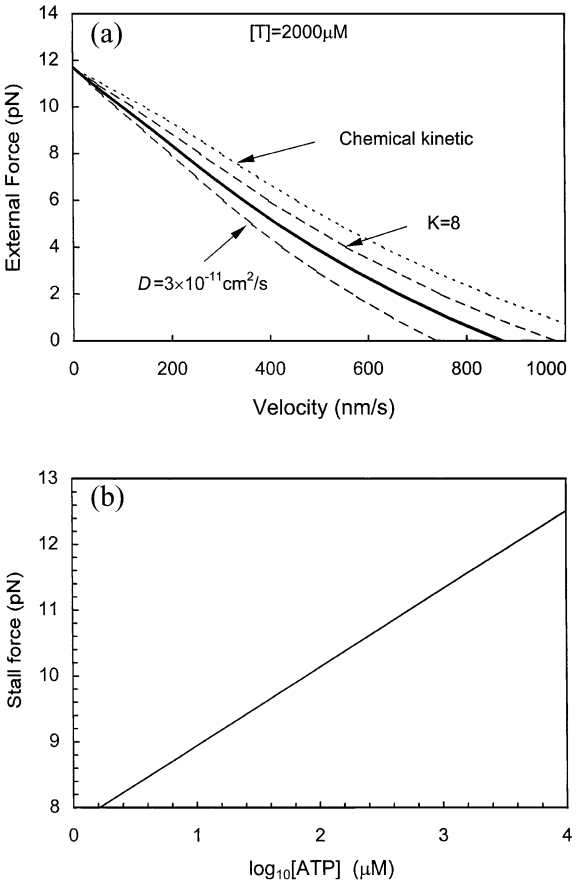

Fig. 4. (a) The force–velocity curve calculated as a function of the external load using the standard set of parameters in Table 1 (solid line). The two dashed curves are obtained for reduced K and D, separately. The dotted curve is evaluated using the pure chemical formalism. (b) The stall force calculated for the model using the parameters in Table 1 is plotted as a function of the ATP concentration. The same curve is obtained when the stall force is evaluated using the pure chemical formalism or when any of the hydrodynamic parameters is altered.

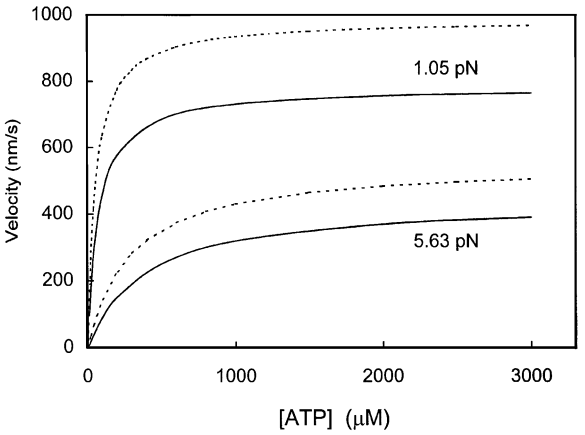

Fig. 5. Bead velocities calculated for the model using the exact formalism of this paper (solid lines) and the chemical formalism (dashed lines) are plotted as a function of the ATP concentration in solution for $\bar{F} = 1.05$ and 5.63 pN.

the force–velocity curves in Fig. 4a by extrapolation. As shown in Fig. 4a, all the force–velocity curves intercept the y-axis at the same point. This implies that the stall force of this model should not depend on the values of the hydrodynamic parameters of the system, nor on whether it is evaluated using our formalism or the chemical formalism. Fig. 4b shows the calculated stall force as a function of ATP concentration for the model.

4.4. Effect of ATP concentration

In Fig. 5, the bead velocity as a function of [ATP] is evaluated for two values of $\bar{F}$ using both the present and the chemical formalisms. It is easy to see that each individual curve has the characteristic shape of the Michaelis–Menten kinetic curve:

$$\bar{u} = \bar{u}_{\max}[\mathrm{ATP}]/([\mathrm{ATP} + K_{\mathrm{m}}]) \tag{21}$$

However, similar to the force–velocity curve in Fig. 4a, the mean velocity of the motor evaluated from the chemical formalism is also always larger than those evaluated from the present formalism. That is, neglecting the force fluctuation in the elastic element (due to the movement of the bead) always overestimates the value of the veloc-

ity of the motor. Although it is obtained based on the simple two-state model, we expect this conclusion to be generally applicable to any hand-over-hand model, because of the non-linear properties of the rate constants in Eqs. (2)–(5) (see below).

5. Discussion and conclusions

The key step of the present formalism is to solve Eqs. (12) and (13) using equations in Eqs. (14)–(19). These two equations can be solved numerically when the basic kinetic rate constants of the model, $\bar{k}_+^{\alpha}$, etc., in Fig. 1a, are given (as in Table 1). Although it was derived based on the tight-coupled two-state model in Fig. 1a, the formalism can be easily extended to models with slippage (loose-coupled) or to models with more than two states in the kinetic mechanism. Since it deals directly with the dynamics of the bead, the formalism can be used directly to interpret or study the measured mechanical data obtained from the motility assay. For example, the formalism is especially useful in analyzing the 'frictional' force–velocity curve obtained by varying the viscosity of the medium as measured by Hunt et al. [4]. However, it is important to point out that only the mean velocity or the mean ATP hydrolysis rate of the motor can be evaluated using the present formalism. To evaluate properties of the motor related to fluctuations, such as the randomness parameter [10], one has to use the Monte Carlo method [27–29].

Recently, Elston and Peskin [30] presented a theoretical study on the same motility assay, also focusing on the movement of the bead. However, their system is quite different from ours in that they used the 'Brownian Ratchet' mechanism for the movement of the kinesin motor on microtubule. In our system, the kinesin motor translocates on microtubule through binding and unbinding and conformational changes of the two heads, a mechanism similar to the 'crossbridge' model used in muscle contraction [25,31,32].

As one can see from Fig. 2a,b, and Fig. 3a, the velocity of the bead in the motility assay at a given load and ATP concentration depends on the 'mobility' of the bead in the assay: the more mobile the bead, the larger the velocity. Thus, experimentally one could increase the velocity of the bead by decreasing the elasticity of the elastic element connecting the bead and the motor or by increasing the diffusion coefficient of the bead by decreasing the size of the bead or the viscosity of the medium.

It is important to point out that the stall force evaluated for the present two-state model is found to be independent of the hydrodynamic parameters of the system. Thus, it is not surprising to find that the frictional-force–velocity curve is identical to the external-load–velocity curve (compare Fig. 3b and Fig. 4a). The stall force evaluated using the chemical formalism is also found to be identical to that evaluated using our formalism. All these phenomena are the direct result of the assumption that the coupling between the ATP hydrolysis and the translocation of the motor on the microtubule is tight in this model. That is, the motor cannot slip, nor completely dissociate from the lattice. As a result, when the motor stalls, the force received by the motor is always equal to the load applied to the bead, independent of the stiffness of the elastic element or the size of the bead, etc., and the system is at a thermodynamic equilibrium. If the motor can dissociate from the lattice (loose coupling), the system is at a steady state, not equilibrium, when the bead movement is stalled. In this case, the stall force is critically dependent on the hydrodynamic parameters of the system, as found in the one-headed motor case [1]. Thus, by measuring the stall force at different hydrodynamic conditions one may be able to assess whether the motor can slip or dissociate completely from the microtubule during the execution of the catalytic cycle.

As shown in Fig. 4a and Fig. 5, the velocity of the bead for the two-state model evaluated from our formalism was found to be smaller than that from the chemical formalism. That is, with the same set of kinetic parameters, the turnover rate of ATP hydrolysis of the motor evaluated from our formalism is always lower than that evaluated from the chemical formalism. This result indicates that the hydrodynamic relaxation and Brownian motion of the bead do have a great effect on the kinetic behaviors of the motor. The only time

that the movement of the bead has no effect on the kinetic behavior of the motor is when the elastic element is completely flexible.

In conclusion, we have developed a formalism that directly deals with the dynamic behavior of the bead in the motility assay of Visscher et al. [10]. In this motility assay, a large bead (much larger than the motor) is attached with a single two-headed motor and the movement of the bead (not the motor) under a constant load powered by the motor is measured. Mathematical equations are derived that can be used to evaluate the velocity of the bead in the assay when the kinetic mechanism of the motor is given. Since it deals directly with the movement of the bead, the formalism is especially useful in analyzing motility data that depend on the hydrodynamic parameter of the bead, such as the size of the bead or the viscosity of the medium, etc. We showed that the velocity of the bead calculated from the pure chemical formalism is larger than that calculated from our formalism. We also showed that the stall force measured as a function of the hydrodynamic parameters of the system could be used to tell whether the coupling between the ATP hydrolysis and the movement of the motor on microtubule is tight or loose.

References

[1] Y. Chen, Theoretical formalism for kinesin motility I. Bead movement powered by single on-headed kinesins, Biophys. J. 78 (2000) 313–321.

[2] J.A. Howard, A.J. Hudspeth, R.D. Vale, Movement of microtubules by single kinesin molecules, Nature 342 (1989) 154–158.

[3] S.M. Block, L.S. Goldstein, B.J. Schnapp, Bead movement by single kinesin molecules studied with optical tweezers, Nature 348 (1990) 348–352.

[4] A.J. Hunt, F. Gittes, J. Howard, The force exerted by kinesin against a viscous load, Biophys. J. 67 (1994) 766–781.

[5] K. Svoboda, S.M. Block, Force and velocity measured for single kinesin molecules, Cell 77 (1994) 773–784.

[6] E. Meyhofer, J. Howard, The force generated by a single kinesin molecule against an elastic load, Proc. Natl. Acad. Sci. USA 92 (1995) 574–578.

[7] R.D. Vale, T. Funatsu, D.W. Pierce, L. Romberg, Y. Harada, T. Yanagida, Direct observation of single kinesin molecules moving along microtubules, Nature 380 (1996) 451–453.

[8] M.J. Schnitzer, S.M. Block, Kinesin hydrolyses one ATP per 8-nm step, Nature 388 (1997) 386–390.

[9] W. Hua, E.C. Young, M.L. Fleming, J. Gelles, Coupling of kinesin steps to ATP hydrolysis, Nature 388 (1997) 390–393.

[10] K. Visscher, M.J. Schnitzer, S.M. Block, Single kinesin molecules studied with a molecular force clamp, Nature 400 (1999) 184–189.

[11] H. Qian, A simple theory of motor protein kinetics and energetics, Biophys. Chem. 67 (1997) 263–267.

[12] H. Qian, A simple theory of motor protein kinetics and energetics. II, Biophys. Chem. 83 (2000) 35–43.

[13] A.B. Kolomeisky, B. Widom, A simplified 'Ratchet' model of molecular motors, J. Stat. Phys. 93 (1998) 633–645.

[14] M.E. Fisher, A.B. Kolomeisky, The force exerted by a molecular motor, Proc. Natl. Acad. Sci. USA 96 (1999) 6597–6602.

[15] M.E. Fisher, A.B. Kolomeisky, Molecular motors and the forces they exert, Physica A 274 (1999) 241–266.

[16] M.J. Schnitzer, K. Visscher, S.M. Block, Force production by single kinesin motors, Nat. Cell Biol. 2 (2000) 718–723.

[17] J. Gelles, E. Berliner, E.C. Young, H.K. Mahtani, B. Perez-Ramirez, K. Anderson, Structural and functional features of one- and two-headed biotinated kinesin derivatives, Biophys. J. 68 (1995) 276S–281S.

[18] C.S. Peskin, G. Oster, Coordinated hydrolysis explains the mechanical behavior of kinesin, Biophys. J. 68 (1995) 202S–210S.

[19] W.O. Hancock, J. Howard, Kinesin's processivity results from mechanical and chemical coordination between the ATP hydrolysis cycles of the two motor domains, Proc. Natl. Acad. Sci. USA 96 (1999) 13147–13152.

[20] L. Romberg, D.W. Pierce, R.D. Vale, Role of the kinesin neck region in processive microtubule-based motility, J. Cell Biol. 140 (1998) 1407–1416.

[21] T.L. Hill, Free Energy Transduction in Biology, Academic Press, New York, 1977.

[22] H-X. Zhou, Y. Chen, Chemically driven motility of Brownian particles, Phys. Rev. Lett. 77 (1996) 194–197.

[23] T.C. Elston, C.R. Doering, Numerical and analytical studies of nonequilibrium fluctuation-induced transport processes, J. Stat. Phys. 83 (1996) 359–383.

[24] R.A. Alberty, Effect of pH and metal ion concentrations on the equilibrium hydrolysis of adenosine triphosphate to adenosine diphosphate, J. Biol. Chem. 243 (1968) 1337–1343.

[25] E. Eisenberg, T.L. Hill, Y. Chen, Cross-bridge model of muscle contraction. Quantitative analysis, Biophys. J. 29 (1980) 195–227.

[26] D.D. Hackney, The kinetic cycles of myosin, kinesin, and dynein, Annu. Rev. Physiol. 58 (1996) 731–750.

[27] Y. Chen, T.L. Hill, Theoretical calculation methods for kinesin in fast axonal transport, Proc. Natl. Acad. Sci. USA 85 (1988) 431–435.

[28] S. Leibler, D.A. Huse, Porters versus rowers: A unified stochastic model of motor proteins, J. Cell Biol. 121 (1993) 1357–1368.
[29] T. Duke, S. Leibler, Motor protein mechanics: A stochastic model with minimal mechanochemical coupling, Biophys. J. 71 (1996) 1235–1247.
[30] T.C. Elston, C.S. Peskin, The role of protein flexibility in molecular motor function: coupled diffusion in a tilted periodic potential, SIAM J. Appl. Math. 60 (2000) 842–867.
[31] T.L. Hill, Theoretical formalism for the sliding filament model of contraction of striated muscle, Prog. Biophys. Mol. Biol. 28 (1974) 267–340.
[32] A.F. Huxley, Muscle structure and theories of contraction, Prog. Biophys. Biophys. Chem. 7 (1957) 255.